

We are IntechOpen, the world's leading publisher of Open Access books Built by scientists, for scientists

5,500

Open access books available

136,000

International authors and editors

170M

Downloads

Our authors are among the

154

Countries delivered to

TOP 1%

most cited scientists

12.2%

Contributors from top 500 universities



WEB OF SCIENCE™

Selection of our books indexed in the Book Citation Index
in Web of Science™ Core Collection (BKCI)

Interested in publishing with us?
Contact book.department@intechopen.com

Numbers displayed above are based on latest data collected.
For more information visit www.intechopen.com



Early Predictive Biomarkers for Hypertension Using Human Fetal Astrocytes

*Fahmida Abdi, Ann M. Simpson, Sara Lal
and Kaneez Fatima Shad*

Abstract

Hypertension is a major risk factor for cardiovascular and cerebrovascular diseases, causing high numbers of deaths and /or disabilities worldwide. Previous studies have reported numerous biomolecules, such as, triglycerides and fibrinogen as biomarkers of hypertension (HTN), but none of these biomolecules could be considered as 'true' predictive biomarkers as they were produced after the establishment of HTN. Therefore, there is an urgent need for identifying and monitoring molecules that are linked to early pre-HTN stages, that is, prior to the onset of HTN. Astrocytes are the most abundant cells in the nervous system and through their long processes, astrocytes can communicate with both neuronal and non-neuronal cells such as endothelial cells lining blood vessels. Thus, any biochemical changes in astrocytes will affect both blood vessels and neurons. We are using human fetal astrocytes (HFAs) to investigate the molecules which may possibly act as early predictive biomarkers for hypertension. Astrocytic processes are mostly supported by the intermediate filaments, an example is the glial fibrillary acidic protein (GFAP) which is a type III intermediate filament. Elevated GFAP levels are being considered as a marker of astroglial injury, indicating the conversion of non-reactive (A2) into reactive (A1) astrocytes. Our initial immunohistochemistry studies using anti-GFAP antibodies on astrocytes from spontaneous hypertensive rats (SHRs) and their normal counter parts (WKY) rats showed a similar profile to that of reactive (A1) and non-reactive (A2) HFAs, respectively. Numerous studies point to a significant role of calcium ion channel proteins in hypertension, and calcium channel blockers such as Amlodipine (Norvasc) Diltiazem (Cardizem) are commonly used as antihypertensive drugs. By using liquid chromatography–tandem mass spectrometry (LC–MS/MS) we observed that reactive (A1) astrocytes, contain more calcium-activated proteins such as calpain, calpastatin, cathepsin and mitogen activated protein kinase (MAPK) as compare to normal (A2) HFAs, suggesting their possible link to the future onset of HTN. Hence these proteins could be considered as potential early predictive biomarkers of HTN.

Keywords: Hypertension, spontaneous hypertensive rats (SHRs), WKY rats, Human fetal astrocytes (HFAs), Reactive (A1) and non-reactive (A2) HFAs, glial fibrillary acidic protein (GFAP), Ca²⁺ dependent proteins, LC–MS/MS technique

1. Introduction

Scientific studies have established that prevalence of hypertension (HTN) needs to be reduced in order to control cardiovascular and cerebrovascular diseases [1]. At present, many laboratories around the world are exploring a plethora of biomarkers, as early indicators of HTN [2, 3], i.e., triglycerides, C-reactive protein, fibrinogen, serum albumin, uric acid, homocysteine and intracellular adhesion molecule-1 (ICAM-1) [4]. All these biomarkers for hypertension are produced as a result of chronic disease-related comorbidities such as atherosclerosis, Type 2 diabetes and renal failure, therefore, they cannot be considered as 'true' predictive biomarkers for hypertension. Hence, this study is focusing on glial fibrillary acidic protein (GFAP), and a group of calcium-dependent proteases, such as calpain, calpastatin, cathepsin and mitogen activated protein kinase (MAPK), known to be strongly associated with HTN; hence could be potential early biomarkers for HTN.

Similarly, an endogenous chemical, N-Methyl-D-Aspartic acid (NMDA), a type of glutamate is also documented as linked with HTN [5]. NMDA is a major excitatory neurotransmitter in the central nervous system, consisting of two types of receptors namely synaptic and extrasynaptic. Research indicates that the activation of the synaptic NMDA receptors is neuroprotective; whereas, the stimulation of extrasynaptic NMDA receptors (NMDARs) promotes cell death [6] and resultant HTN, which can be regulated by NMDA antagonists, such as 1-amino cyclo propane carboxylic acid (ACPC) [7]. NMDA type glutamate receptors are not only present in the neuronal cells but also in the non-neuronal cells such as astrocytes [8]. Recent studies have demonstrated a significant role of astrocytes in regulating blood flow due to the elevation in intracellular calcium (Ca^{2+}) [9], which plays a significant role in the regulation of blood pressure.

Astrocytes are present between blood vessels and neurons and are responsible for changes in the arterial blood pressure [10]. A decline in the cerebral blood supply activates the astrocytes to release a chemical signal to the nearby neurons that raises blood pressure, restoring blood flow and oxygen supply to the brain [10]. Thus, astrocytes perform a balancing role between brain perfusion and neuronal activities by mobilising their internal calcium [11], which in turn triggers the release of chemical transmitters such as glutamate [12]. Consequently, there is a calcium-dependent bidirectional signalling pathway between astrocytes and neurons [13], which opens up the possibility of astrocytic involvement in the modulation of calcium-dependent molecules such as calpain, calpastatin, cathepsin and MAPK, which can potentially be considered as direct predictive biomarkers of HTN.

Certain behavioural conditions, such as, stress also elevates blood pressure. Under stressful conditions, excessive release of corticotropin-releasing hormone (CRH) activates NMDA receptors, resulting in an influx of Ca^{2+} molecules, which enhance the activity of m-calpain [14]. Calpain is one of the major calcium-dependent proteolytic enzymes with various isoforms such as μ -calpain and m-calpain, which are activated by the synaptic and extra-synaptic NMDA receptors respectively [15, 16]. Studies have indicated that the activation of μ -calpain is important for cell-survival, whereas the stimulation of m-calpain initiates toxic effects and cell death [6], due to its interaction with NMDAR [17]. Activation of the type of NMDA receptor defines the communication from the synapse to the nucleus [18].

Stimulation of synaptic NMDAR phosphorylates the intermediate filament proteins by extracellular signal regulated kinases 1 and 2 (ERK1/2) [19]. However, the activation of extrasynaptic NMDAR fails to phosphorylate and translocate intermediate filament proteins into the nucleus. The phosphorylated or non-phosphorylated state of intermediate filament proteins determine whether it promotes cell survival or induces cell death. These diverse functions that require the regulation

of gene and synapse-to-nucleus communications are controlled by nuclear calcium signalling [20]. Overexpression of these proteins induces neurodegeneration, whereas, its suppression has the opposite effect, therefore, the molecules that keep the balance may act as therapeutic targets for HTN.

To date, most proteomic research, targeted at discovering biomarkers, has failed to incorporate adequate biomarker validation studies in independent sample sets. These are necessary steps in the translation of potential biomarkers into clinical practice. Recent development of sophisticated mass spectrometry-based quantitation of multiple proteins has enabled the validation of candidate biomarkers in different biological materials, such as astrocytes.

The literature indicates that reactive astrocytes (A1) and their intermediate filaments contain greater concentrations of glial fibrillary acidic protein (GFAP) [21], compared to normal astrocytes (A2). The purpose of this study was, to identify and quantify the differences between the proteins of interest, present in the reactive and the normal human foetal astrocytes (HFAs), using immunocytochemistry and single-pot, solid-phase-enhanced sample-preparation (SP3) [22] proteomic techniques. We aim to detect the immunocytochemical differences between the A1 and A2 HFAs using GFAP antibodies and to identify a panel of protein biomarkers in A1 and A2 HFAs for the prediction of hypertension.

2. Materials and methods

2.1 Ethical approval

HFAs were obtained from the Biobank of Macquarie University, after approval from the UTS Human Research Ethics Committee (ETH17-1883).

2.2 Protocol for the cell culture of primary HFAs

After getting a material transfer agreement (MTA # 17/979) between the two universities, the HFAs were tested for mycoplasma contamination and were found to be negative. The HFAs were then cultured in T75 flasks using Roswell Park Memorial Institute (RPMI 1640) media containing 10% heat-inactivated foetal calf serum (FCS) (**Table 1**), at 37°C, in a 5% CO₂ humidified incubator. Freshly prepared media was used to feed the cells every five days.

The HFAs were seeded at 4×10^7 cells/T75-cm² in tissue culture flasks containing RPMI (4.5 g/L glucose, L-glutamine, and 25 mM HEPES buffer), plus 10% FCS at 37°C, and incubated in a 5% CO₂ humidified incubator.

For re-seeding, HFAs were detached from the flask by using 4 ml of trypsin, incubated for 3 minutes at 37°C, in a 5% CO₂ humidified incubator. After incubation with trypsin, the cells were transferred to a 15 ml falcon tube and were centrifuged at 1600 g rpm, for 3 minutes. Trypsin was removed by washing three times with phosphate buffered saline (PBS). The cells were then resuspended in 2 ml of fresh media by gentle mixing and 1 ml of this cell solution was added to each T75 flask with 14 ml RPMI, labelled as A1 and A2 for reactive and normal astrocytes, respectively.

2.3 Conversion of normal HFAs (A2) into reactive HFAs (A1)

After achieving 95 to 100% confluency and three days before the proteomics experiment, the HFAs were incubated in the RPMI media with 1% FCS instead of 10% FCS, to avoid false positive proteomic results due to the proteins present in the 10% FCS. Twenty-four hours before the pellet formation for SP3 [22] protocol,

S. N.	Chemical	Catalogue number	Company	Amount used	Quantity T75 flask
1	RPMI 1640	11875	Thermo Fisher Scientific	45 ml	15 ml of complete media
2	Foetal Calf Serum	A3160401	Thermo Fisher Scientific	5 ml	
3	Trypsin	9035-81-8	Sigma-Aldrich		4 ml
4	Phosphate-buffered saline (PBS)	10010023	Thermo Fisher Scientific		3 ml
5	Adenosine 5- triphosphate disodium salt hydrate (ATP)	34369-07-8	Sigma-Aldrich		100 µl
6	Paraformaldehyde	30525-89-4	Sigma-Aldrich	4% paraformaldehyde in PBS, with 7.4 pH	1 ml

Table 1.
Chemicals used for the tissue culture experiments.

the cells were returned to RPMI media +10% FCS in both A1 and A2 flasks. Then, 100 µl of 1 mM adenosine triphosphate (ATP) was added to the A1 flask to convert the normal HFAs into reactive HFAs [23]. After 24 hours of incubation at 37°C, in a 5% CO₂ humidified incubator, the cells were washed three times with PBS. The cells were subsequently detached from both flasks by adding 4 ml of trypsin and were incubated at 37°C in a humidified incubator, for 3 minutes. After incubation, the cells were transferred into two falcon tubes (15 ml tubes, labelled as A1 and A2) and were centrifuged at 1600 g rpm for 3 minutes. Trypsin was removed from the tubes by washing three times with 3 ml PBS. The cell samples from both tubes were transferred into 2 ml Eppendorf tubes and were microfuged for 1 minute, to remove PBS. Subsequently, the Eppendorf tubes containing cell pellets were snap frozen in liquid nitrogen and stored at -80°C for the proteomics experiment, using SP3 protocol.

2.4 Immunocytochemistry of HFAs using anti-GFAP stain

Six poly-L-lysine coated coverslips, three labelled as A1 and three as A2 were placed in a six well plate, containing 2 ml of fresh RPMI media with 10% FCS. The plates were incubated at 37°C, in a 5% CO₂ humidified incubator to grow until ~70% confluency was achieved.

The cells in three of the six wells, were treated with 1 mM ATP to convert them into reactive (A1) astrocytes, whereas the other three coverslips with the HFAs (A2) were not treated with ATP. After 24 hours of incubation all the cells were washed three times with 0.1 M PBS, fixative (4% paraformaldehyde in PBS, 7.4 pH) was then added for 30 minutes, at room temperature. After fixation, both types of HFAs were gently washed three times with PBS and were ready for permeabilization and blocking of the unspecific binding of the proteins. To improve the permeabilization of the antibodies, the HFAs were incubated with 100 µl of 0.1% Triton X 100, for 30 minutes, at 37°C, in a 5% CO₂ humidified incubator. The cells were gently washed three times with PBS, before being treated with the blocking solution (100 µl of 5% goat serum) and then the cells were incubated for 30 minutes.

The cells were incubated with a primary anti-GFAP antibody (1:100 dilution, ab7260 from ABCAM) at 4°C for 18 hours. Then, the HFAs were washed three times with PBS, and were incubated with the secondary antibody (1:100, ab150077 with AF488, ABCAM) in 1% BSA for 1 hour at the room temperature in the dark.

2.4.1 Nuclear staining and mounting

The HFAs were rinsed with PBS and were incubated with 1 µg/ml of nuclear stain [4, 6-diamidino-2-phenylindole (DAPI)] for 10 minutes followed by three rinses with PBS. Excess PBS was carefully wiped around the coverslips and the cells were mounted on the glass slides (75 mm x 25 mm and 1 mm thickness), which were clearly labelled with the type of cell and stain. Then a drop of mounting medium, Fluoroshield (ABCAM) was placed in the middle of the slide. The coverslip with the stained cells was carefully lifted using forceps and was placed in an inverted position on top of the slide, air bubbles were removed, and the cells were sealed with a clear nail polish to prevent drying and movement under the microscope. The cells were stored in the dark, at +4°C till image analysis was performed using the NIKON A1 confocal microscope.

2.5 Protein extraction and digestion using single-pot, solid-phase-enhanced sample-preparation (SP3) protocol

The proteins of interest were extracted from A1 and A2 HFAs using the SP3 protocol, before performing mass spectrometric analysis. All the chemicals and equipment used for the preparation of lysis buffer and for protein extraction and digestion using SP3 protocol are shown in **Table 2** and **Figure 1**.

Chemical name	Company	Cat. No.
Bovine serum albumin (BSA)	Sigma	00A2153
Sodium dodecyl sulfate (SDS)	Bio-Rad	1610302
Triton X-100	Sigma	T8787
Nonidet-P40 (NP-40)	Merck-Millipore	492016-100ML
Tween 20	Sigma	P1379
Deoxycholate	Sigma	3970
Sodium chloride (NaCl)	Sigma	S7653
Glycerol	Sigma	G5516
HEPES sodium salt	Sigma	H3375
Iodoacetamide	Bio-Rad	1632109
Dithiothreitol (DTT)	Bio-Rad	1610611
Ammonium bicarbonate	Sigma	A6141
Trypsin + rLysC mix	Promega	V5073
1.5-mL Safe-Lock tubes	Eppendorf	22363204
Tris-2-carboxyethyl phosphine	Sigma	51805-45-9
Sera-Mag Speed Beads	GE Healthcare	45152105050250
Magnetic rack, Magnetic Sphere	Promega	Z5342

Table 2.
 Reagents and equipment used for SP3 protocol.



Figure 1.

The magnetic rack used for placing the sample-vials containing magnetic beads. When vials are placed on the magnetic rack, the beads start to stick to the wall of the vial. This process allows the protein molecules to attach safely to the beads, so unwanted fluid could be easily discarded.

2.5.1 Preparation of reconstitution (lysis) buffer for SP3

Reconstitution buffer was freshly prepared by mixing 100 μl of each of the following chemicals, i.e., 10% SDS, 10% Triton x-100, 10% NP-40, 10% Deoxycholate and 10% Glycerol. In addition, 10 μl of 5 M NaCl, 20 μl of HEPES (pH 8.0) and 470 μl of water was added to the mixture.

2.5.2 Extraction of the proteins from A1 and A2 HFA samples

Eppendorf tubes containing pellets of A1 and A2 astrocytes were removed from -80°C and were resuspended in 50 μl of lysis buffer. To facilitate the extraction process, the tubes were heated to 90°C on the heating block for 10 minutes. To reduce the number of disulfide bonds, 1 μl Tris 2-carboxyethyl phosphine (TCEP) was added to the samples, followed by 1 μl of acrylamide monomer to alkylate the mixture. After an hour of incubation at room temperature, the alkylation reaction was stopped by adding 1 μl of dithiothreitol (DTT). Before extracting the proteins from both types of HFAs, a standard curve was constructed using an ampule of 2 mg/ml bovine serum albumin (BSA).

2.5.3 Construction of the standard curve

The standard curve was constructed using a 96 well microplate, and bovine serum albumin (BSA) was added at a concentration ranging from 0 to 2000 $\mu\text{g}/\text{ml}$ diluted with double distilled water. Similarly, A1 and A2 sample solutions were also diluted with double distilled water at a ratio of 1:10 & 1:20. Working solution of BCA was prepared by adding reagent B (cupric sulfate) with reagent A (cuprous sulfate), at a ratio of 1:50. The plates were prepared according to **Table 3**. Nine wells of the plate were filled with 25 μl of BSA solution ranging from 0 to 2000 $\mu\text{g}/\text{ml}$ along with the blank and two dilutions of A1 and A2 samples. Then 200 μl of working solution was added in each of the fourteen wells. The plates were covered with parafilm and were incubated at 37°C for 30 minutes, and the plates were read on the Tecan Infinite 200 Pro, spectrophotometer, at a wavelength of 562 nm, using Magellan software.

S.N.	Vial volume of diluent (μl)	Volume and source of BSA (μl)	BSA concentration ($\mu\text{g/ml}$)
A	0	300 of Stock	2000
B	125	375 of Stock	1500
C	325	325 of Stock	1000
D	175	175 of vial B dilution	750
E	325	325 of vial C dilution	500
F	325	325 of vial E dilution	250
G	325	325 of vial F dilution	125
H	400	100 of vial G dilution	25
I	400	0	Blank
Samples			
A1(1:10)	9	1	38
A1(1:20)	19	1	26
A2(1:10)	9	1	22
A2(1:20)	19	1	18

Table 3.
 Dilution scheme protocol for standard in vials (work-range, 25–2000 $\mu\text{g/mL}$).

Data obtained was used to plot a standard curve and the concentration of the proteins in the A1 and A2 astrocyte samples were determined from **Figure 2**.

2.5.4 Reconstitution of the proteins from A1 and A2 samples

The cell-solution was diluted to a final volume of 48 μl by adding double distilled water and 2 μl of hydrophilic magnetic beads to the samples, giving a total volume of 50 μl of protein solution. Proteins were bonded with the beads by adding 50 μl of 100% ethanol to the above mixture and vortexed for 5 minutes. Hydrophilic magnetic beads, were coated with carboxylate functional groups to capture the proteins, making it easier to wash the cells in 100% ethanol. Surfactant was removed by rinsing the cells three times with 80% ethanol and the supernatant with unbound

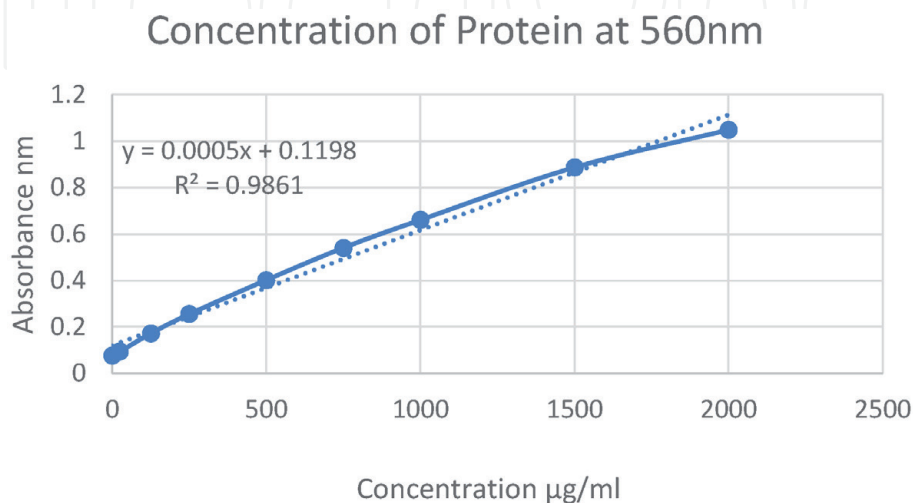


Figure 2.
 BCA (Bicinchoninic acid) protein assay was used to plot standard curve for quantitation of the protein concentrations in the A1 and A2 astrocytes.

compounds was discarded in a waste container. Proteins were extracted in aqueous solution by adding 100 μ l of 200 mM ammonium bicarbonate to the protein bonded beads. Trypsinisation of proteins was achieved by incubating the samples overnight with 1 μ l of trypsin at 37°C.

2.5.5 STop and go extraction (STAGE) tips protocol

Further desalting and cleaning of the peptides was performed by an extended protocol called STop and Go Extraction (STAGE) tips protocol [22]. The first step was to prepare Styrenedivinylbenzene-reverse phase sulfonated (SDB-RPS) for the process of solid phase extraction. Briefly, a large sized SDB-RPS disk was placed in a covered petri dish and from that a 47 mm disk core was used in this protocol as a solid phase extraction sorbent. These sorbents have a high affinity for polar organic compounds, and hence reduce the extraction time and solvent, used for analytical preparation of aqueous environmental samples.

2.5.6 Construction of STAGE tip and preparing of collection tubes

STAGE tip (**Figure 3**) was prepared by using a flat-ended needle, to push the 47 mm SDB-RPS core carefully inside a 2 ml pipette-tip, keeping it 2–3 mm above its end. A hole was made in the middle of the lid of a 2 ml Eppendorf tube using a rotary cutting tool. The pipette tip with SDB-RPS disk was inserted into the Eppendorf tube through the hole. Double distilled water was used to make 10% v/v trifluoroacetic acid (TFA), then 90% of isopropanol was added to make 1% TFA and this was diluted 1:10 with water. Fresh elution solvent was made by mixing 700 μ l of Acetonitrile, 71 μ l of NH_4OH stock and 229 μ l of water.

2.5.7 Desalting and washing the samples

The sample was acidified by adding 10 μ l of 10% TFA and was centrifuged for 5 minutes at maximum speed. Using one STAGE tip, the sample was pipetted into the top of the tip and centrifuged at 5000 g rpm for 1 minute. The tubes were repeatedly centrifuged until all the liquid passed through the STAGE tip. To wash the sample, 60 μ l of 1% TFA was pipetted into the STAGE tip and centrifuged at 5000 g rpm for 2 minutes. Tubes were centrifuged three times to clear all the salts and contaminants from the bound peptides and the liquid in the collection tube was discarded.

2.5.8 Setting up STAGE tip in autovial insert and elution of peptides

For each sample, a separate autovial was used and a yellow spacer was placed between the STAGE tip and the collection tube to hold the STAGE tip in the center of the autovial. Elution solvent was prepared by mixing 30 ml of 1 M Ammonium Hydroxide with 70 ml Acetonitrile. To complete the reaction, 60 μ l of elution solvent was pipetted into the STAGE tip and was microfuged for a few seconds to drag the liquid onto the disk, which was incubated on the bench for 10 minutes. The STAGE tip was placed in the insert of the autovial and was centrifuged at 5000 g rpm for 5 minutes. This step was repeated three times to allow all the fluid to pass through the disk into the autovial insert containing all the peptides. For removing all the liquid, the STAGE tip was discarded and the collection tubes with autovial inserts containing peptide samples were placed into the Speed Vac (Thermo Speed Vac Concentrator DNA 120), to vacuum-centrifuge. Then, the autovial inserts were removed from the Speed Vac and the springs were attached back to the bottom of the inserts, before placing them into the autovials. Samples

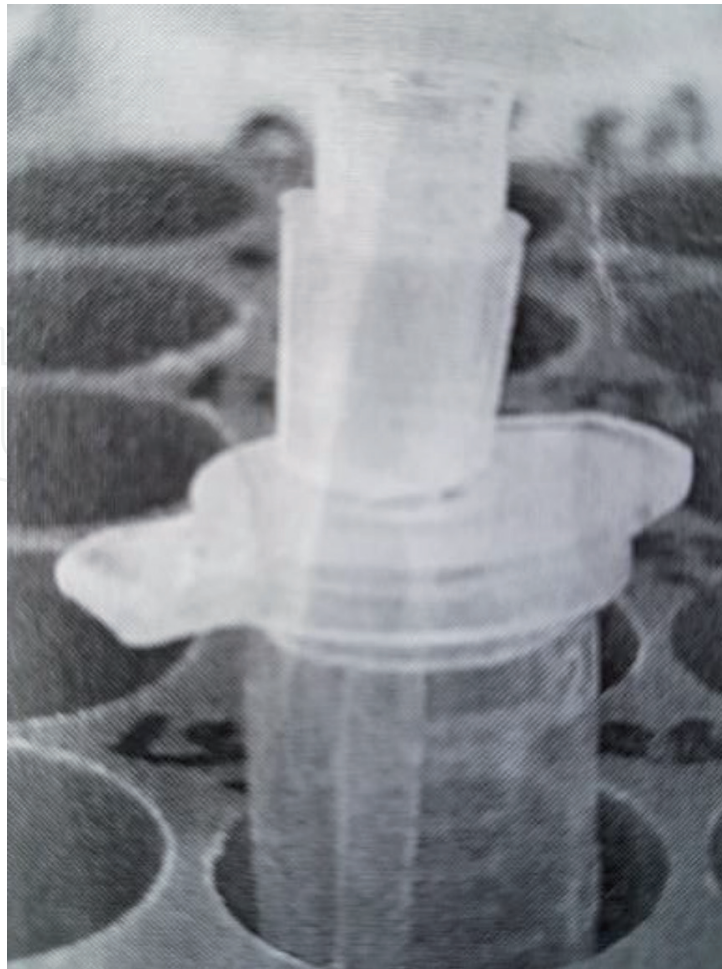


Figure 3.
Shows a 2 ml pipette-tip (STAGE tip) inserted through a hole drilled into the top of a 2 ml collection tube. The pipette tip with SDB-RPS disk was inserted into the Eppendorf tube through the hole. Cell solution was pipetted from the top into tip so peptides could react with the SDB-RPS disk for 10 minutes.

were prepared by adding 25 μ l of MS Loading Solvent-A (2% Acetonitrile +0.1% Trifluoroacetic acid) into each autovial inserts with samples ready to be injected and analysed on mass spectrometer.

2.6 Proteomic data of A1 and A2 HFAs using liquid chromatography – mass spectrometry (LC/MS/ MS) technique

The process of LC/MS/MS technique was optimised with multiple steps using different procedures. The first step of optimisation was the technique used to extract the protein from A1 and A2 HFAs. The following steps were taken to improve the protein extraction from the astrocytes, after analysing the chromatograms (**Figures 4** and **5**), obtained from the proteomics laboratory, UTS.

- i. Clumping of the peptide-peaks was observed due to the effect of surfactant-like substances, as shown in **Figure 4**. Therefore, 1% sodium deoxycholate (SDC) was used as lysis buffer, instead of reconstitution buffer.
- ii. The number of astrocytes for extraction of the proteins was increased from 1×10^6 to 1×10^7 .

The optimisation of protein-elution in relation to the retention time was observed in the following **Figures 4** and **5**.

SP3-01

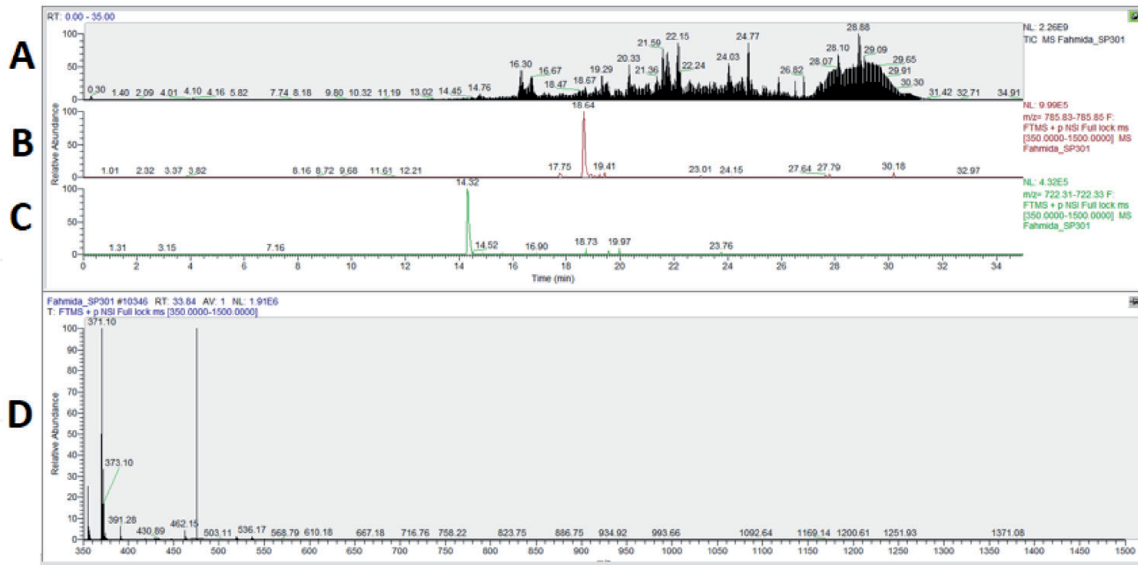


Figure 4.

There were 4 panels in this first set of chromatograms obtained after LC–MS analysis of A1 and A2 astrocytes. Panel A, shows the retention time against frequency of the peptide-peaks, which were clumped together due to surfactant-like substances. Panel B, shows the relative abundance of peptide-spikes against time. Panel C, displays the expanded version of panel B. panel D, indicates mass-to-charge ratio (m/z), used for the standardisation of the other graphs.

SP3-02

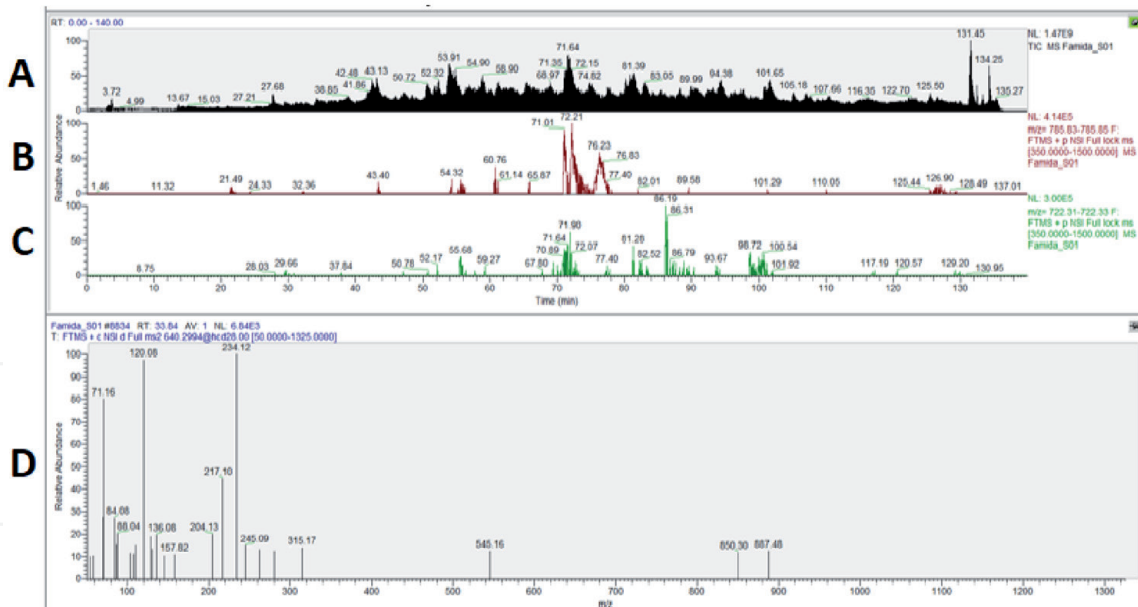


Figure 5.

Panel A, B and C with the same descriptions as for **Figure 4**, except displaying greater retention of protein spikes, because of the optimization of protein extraction method. Panel D, indicates mass-to-charge ratio (m/z), used for the standardisation of other graphs.

2.6.1 PEAKS software

PEAKS (Bioinformatics Solutions Inc.) software was used for the data analysis of the proteins detected from LC–MS–MS, by integrating the area under the curve (**Figure 6**) and statistical comparison of the initial data (**Figure 7**), using Student’s dependent t-test as mentioned below. Triplicates of each set of A1 and A2 samples ($n = 9$) were carefully analysed using either one of the two filters:

- i. Peaks Peptide Score ($-10\lg P$) threshold, only peptides with a score above this threshold were used to quantify the identified proteins, separating low scoring proteins as unique peptide count.
- ii. False discovery rate (FDR) threshold (1%).

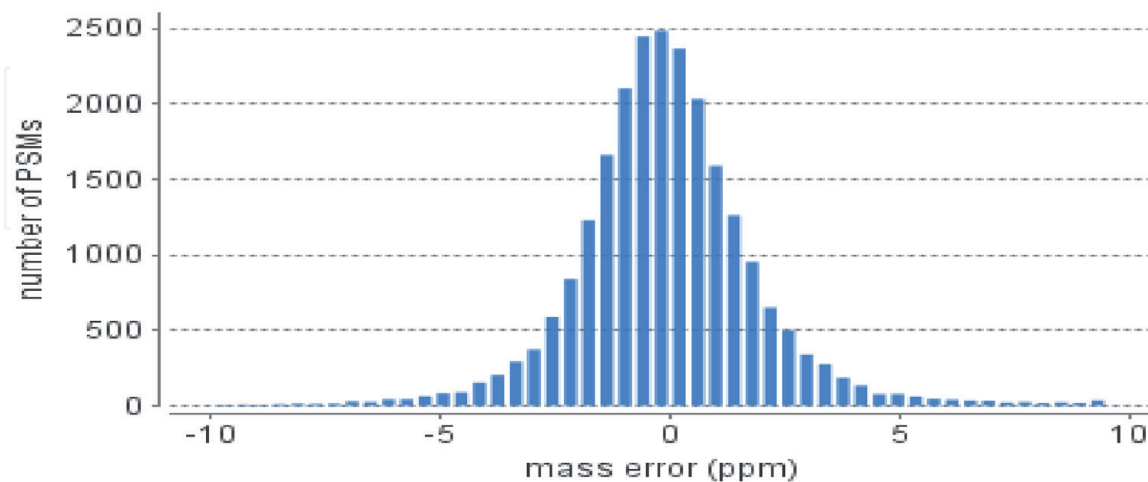


Figure 6. Experimental error chart, indicating the minimal error (1%) in peptides-spectrum matches (PSMs) against part per million (ppm), using PEAKS software.

2.7 Statistical analysis

All values in this text are expressed as mean \pm standard error mean (SEM). Differences between two groups were determined using Student's paired dependent t-test and were considered significant at $P < 0.05$. All statistical analyses were conducted using Microsoft Excel and GraphPad Prism version 8.0.1, GraphPad Software. Light microscopic micrographs were obtained on a Leica Microsystems, LAS version 4.4.0.

3. Results

3.1 A1 (reactive) and A2 (normal) HFAs in culture

The results show that the HFAs increase in size and number with increasing time in tissue culture. Distinct differences were observed in the morphology of the cells present in A1 and A2 flasks, for example A1 astrocytes have more fibroblast-like structures as compared to A2 astrocytes, which look more like neurons (**Figure 7**). A noticeable difference was observed in the thickness of the processes between the two types of the HFAs. This thickening was due to the accumulation of filament proteins such as glial fibrillary acidic proteins (GFAP) as shown in **Figure 8**. Whereas **Figure 9** shows the astrocytes present in the spontaneously hypertensive rat (SHR) and normal Wistar Kyoto (WKY) rat brain slices. **Figure 9**, shows the similarities between A1 HFAs and the SHR astrocytes, implying that the A1 HFAs mimic the hypertensive condition.

3.2 Identification of proteins in A1 and A2 HFAs, using LC/MS/MS technique

The present study was focused on specific proteins, such as glial fibrillary acidic protein (GFAP), calpain, calpastatin, cathepsin and mitogen activated protein kinase (MAPK).

3.2.1 GFAP

The GFAP protein is an indicator of HFAs reactivity, therefore, it was important to carefully measure the area under the curve to determine its degree of intensity. For comparative analysis, the peaks closest to the center of the peptides-spectrum matches (PSMS) were selected, against part per million (ppm) as shown above in **Figure 6**.

The elevated level of GFAP in A1 cells (4.39 ± 0.4) was observed, compared to A2 cells (3.02 ± 0.3), as shown in **Figure 9**. A significantly higher level of GFAP ($P < 0.05$) in A1 compared to A2, resulted in the thickening of processes (indicated by arrows in **Figures 7, 9** and **10** above).

Protein molecules such as calpain, calpastatin, cathepsin and mitogen activated protein kinase (MAPK) are known to be activated by intracellular calcium, leading to their relevant cell signalling cycles and in turn gene [24] modifications.

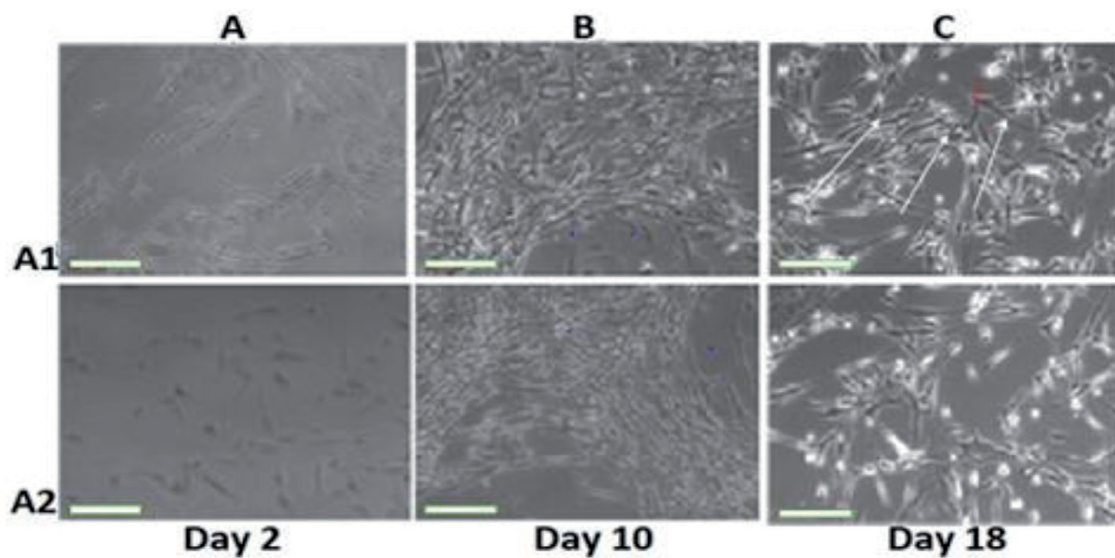


Figure 7. Shows normal HFAs in two flasks, labelled A1 and A2. Panel A and B display 2 and 10 days old normal HFAs, respectively. Panel C, represents 18 days old normal (A2) and ATP-treated reactive (A1) astrocytes, arrows indicating the thickening of the internal filaments. Scale bar, 100 μm .

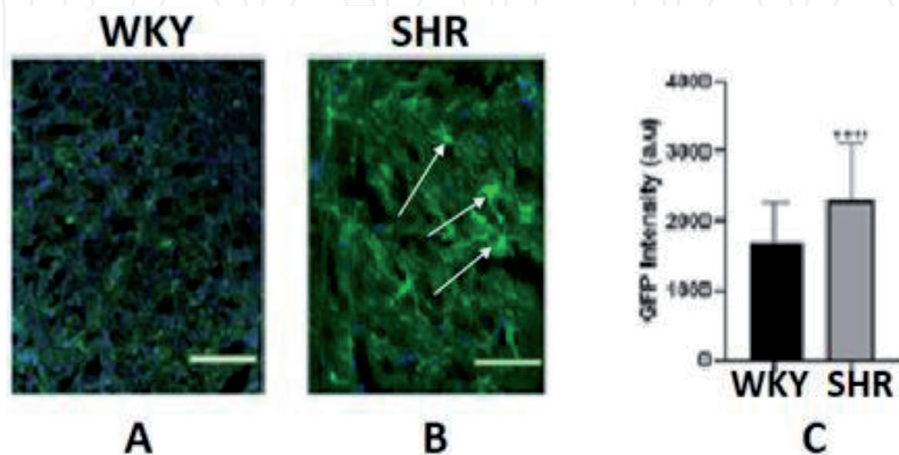


Figure 8. Panel A, shows the normal astrocytes in WKY rat brain slices. Panel B, displays the reactive astrocytes in SHR brain slices. Arrows indicate the upregulation of intermediate filament proteins in SHR astrocytes. Panel C, shows the difference between the intensity of GFAP in the astrocytes of normal and hypertensive rats. *** $P < 0.001$, scale bar, 20 μm .

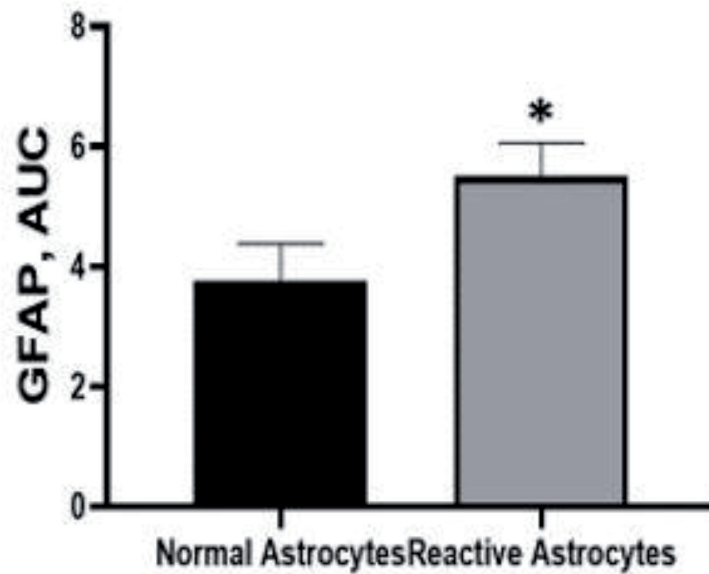


Figure 9.
Level of glial fibrillary acidic protein (GFAP) in normal and reactive astrocytes. Area under the curve (AUC) values are shown as means \pm SEM, * $P < 0.05$, ($n = 9$).

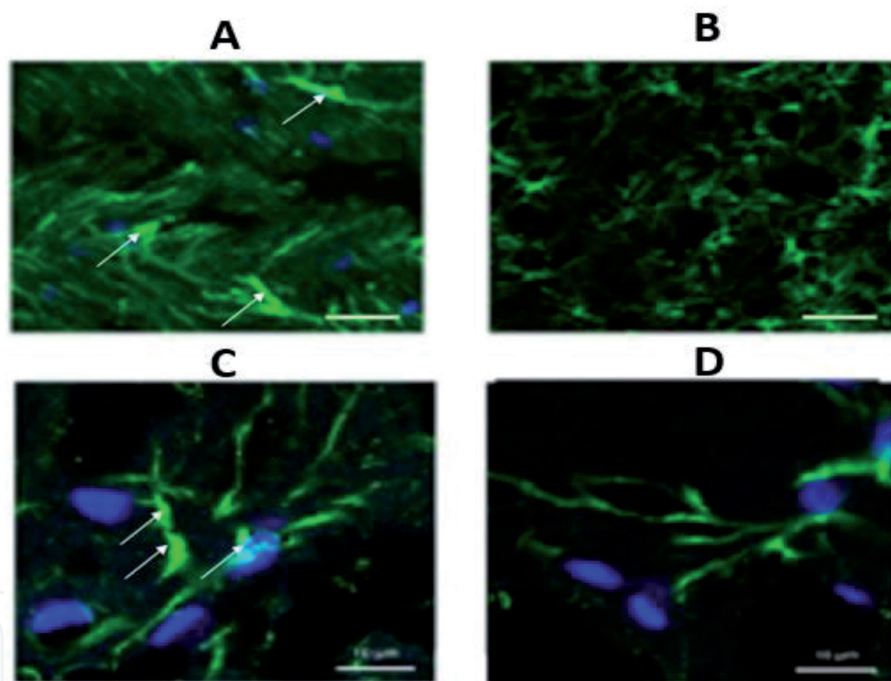


Figure 10.
Panel A (reactive) and panel B (normal) show HFAs after 10 days in culture. Panel C (reactive) and panel D (normal) is after 18 days in culture. Arrows indicate the difference in the thickening of internal filaments, i.e., on day 10 it was $2.5 \mu\text{m}$ as compared to $4.5 \mu\text{m}$ on day 18. Scale bar, $10 \mu\text{m}$.

3.2.2 Calpain

The results show a significantly higher level (**Figure 11**) of Calpain in A1 (6.37 ± 0.6) compared to A2 (3.40 ± 0.2), indicating a greater level of calpain leading to cytotoxicity in reactive HFAs.

3.2.3 Calpastatin

The results indicate that reactive astrocytes A1 (5.52 ± 0.5) have significantly higher levels of calpastatin as compared to the normal A2 (4.09 ± 0.6) astrocytes

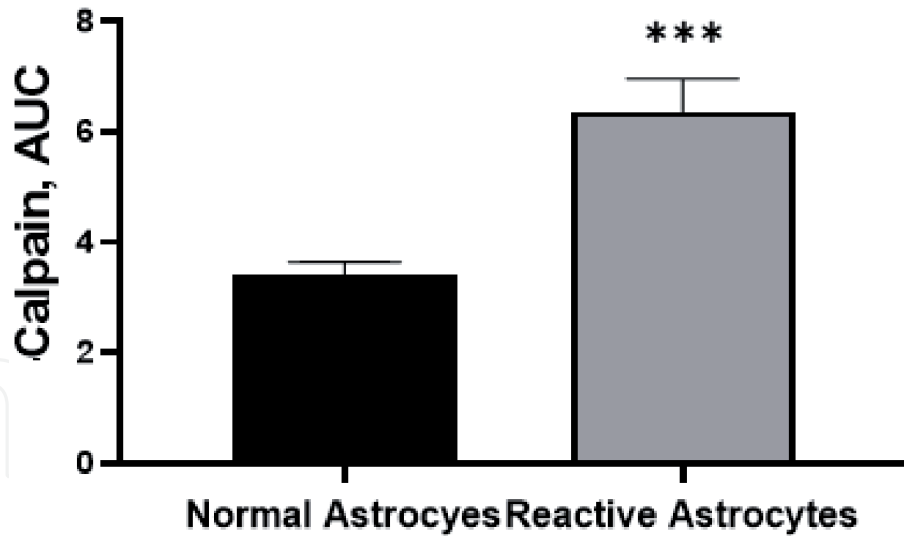


Figure 11. Level of calpain in normal and reactive astrocytes. Area under the curve (AUC) values are shown as means \pm SEM, *** $P < 0.001$, ($n = 9$).

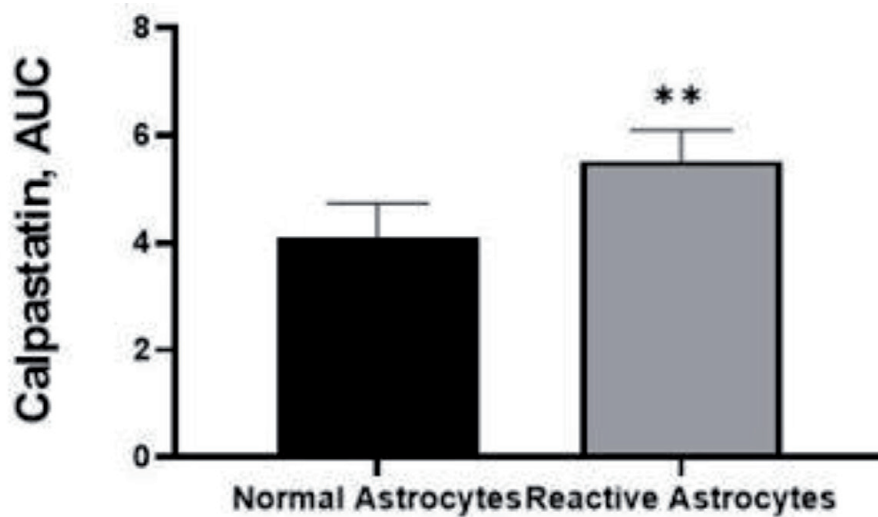


Figure 12. Level of calpastatin in normal and reactive astrocytes. Area under the curve (AUC) values are shown as means \pm SEM, ** $P < 0.01$, ($n = 9$).

(**Figure 12**). Calpastatin is the most specific endogenous calpain-inhibitor, which binds to the active sites of calpain to prevent its activation [25].

3.2.4 Cathepsin

A highly significant increase was observed in the levels of cathepsin in A1 (6.31 ± 0.7) compared to A2 (3.86 ± 0.4) cells (**Figure 13**). Both types of HFAs display human specific cathepsin.

3.2.5 Mitogen activated protein kinase (MAPK)

SP3 Proteomic results show a significantly higher level of MAPK enzyme in A1 (6.31 ± 0.7) compared to A2 (3.72 ± 0.4) HFAs (**Figure 14**). This kinase is an essential component of the cell signalling pathway, responsible for the communication between a receptor on the cell-surface to the DNA inside the nucleus [6, 26].

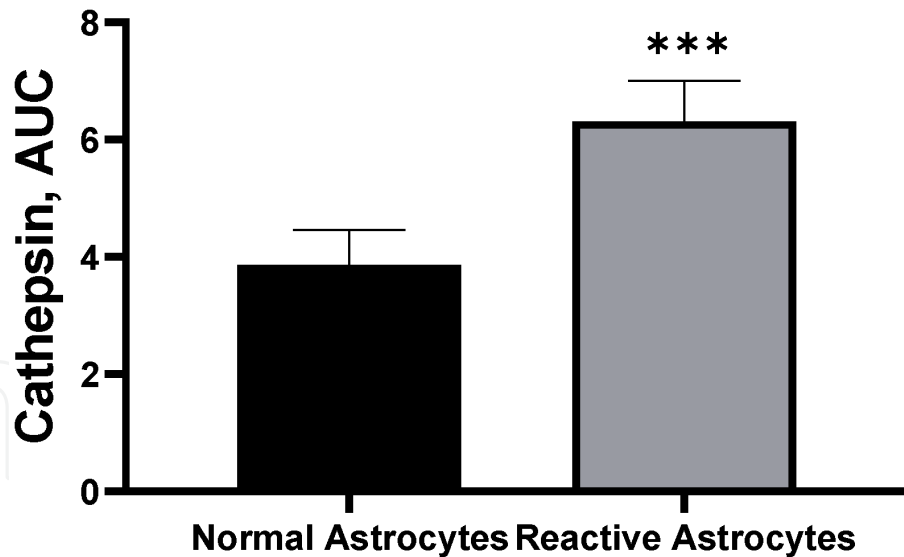


Figure 13.
Level of cathepsin in normal and reactive astrocytes. Area under the curve (AUC) values are shown as means \pm SEM, *** $P < 0.001$, ($n = 9$).

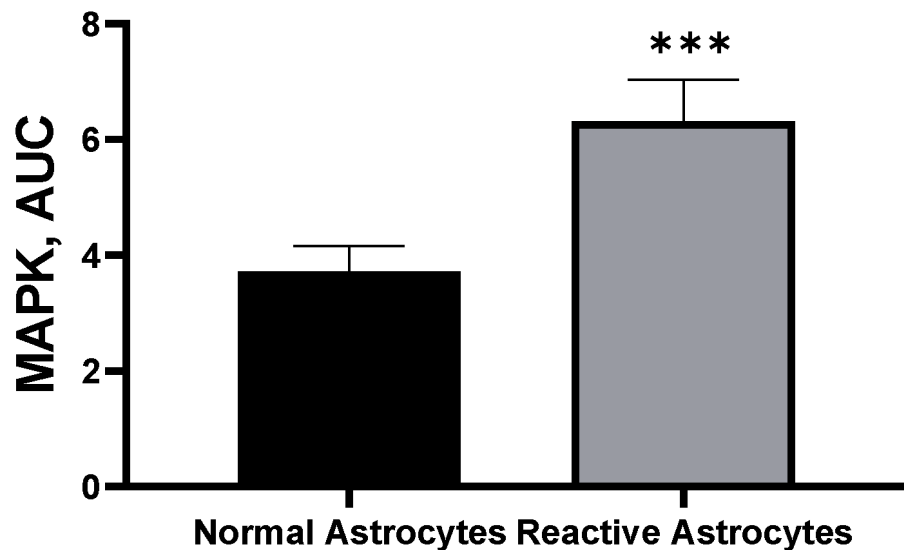


Figure 14.
Level of MAPK in normal and reactive astrocytes. Area under the curve (AUC) values are shown as means \pm SEM, *** $P < 0.001$, ($n = 9$).

All the above-mentioned proteins were identified in both A1 and A2 HFAs, using immunocytochemistry and proteomics (SP3) protocols. Higher levels of calcium-gated proteins in A1 are potential biomarkers of HTN.

4. Discussion

This study demonstrated for the first time that reactive astrocytes in HFAs mimic hypertensive conditions. The present research indicates that the reactive (A1) HFAs have a similar protein profile to astrocytes of hypertensive rats. ATP was used in these experiments to mimic endogenous conditions, as it is released from the damaged cells following tissue injury [27, 28].

The proteins selected as predictive biomarkers for HTN, are either responsible for the reactivity of the astrocytes, or produced because of the interaction between

orexin and NMDA receptors. Most of the proteins selected as predictive biomarkers were calcium binding proteases. The results from A1 and A2 HFAs show that calcium dependent proteins, such as GFAP, calpain, calpastatin, cathepsin and mitogen activated protein kinase (MAPK) were present at higher concentrations in reactive (A1) than in non-reactive (A2) astrocytes. These results suggest that the above-mentioned proteins may be targeted as therapeutic agents for the prevention of HTN.

Immunocytochemistry, in conjunction with the confocal microscopy were used to assess and visualise the proteins, such as internal filament proteins in HFAs. Mass spectrometry (LC/MS/MS) was used to validate the results, obtained by using immunocytochemistry. The SP3 proteomic protocol was employed to identify and estimate the protein-peptide molecules.

Reactive astrocytes (A1) were prepared from the normal (A2) HFAs, by using ATP (**Figure 7**), as described earlier in primary cell lines of neonatal rats [29]. In contrast, a recent research [23] reported that ATP was not sufficient to induce a complete reactive phenotype of astrocytes, in vitro. This discrepancy between the two results may be because HFAs were used in the current study, whereas Adzic et al. [23] used mature astrocytes obtained from the rats. This concept was further verified by the micrographs from light microscopy (**Figure 7**) and confocal microscopy (**Figures 8 and 10**) which showed a gradual increase in the confluency as well as in the thickness of the processes of the HFAs with increasing time in culture. Hence, our experiments confirmed that the reactivity profile of the astrocytes changed as they developed. This proliferation of the filaments is due to an increase in the accumulation of GFAP with time [30]. In A1 astrocytes, the thickness of the processes on day 10 was 2.5 μm as compared to 4.5 μm on day 18 (**Figures 7 and 10**), indicating that there was a periodic increase in the concentration of GFAP in the reactive astrocytes. This significant thickening of astrocytic processes in A1 HFAs (**Figure 8**), was like that observed in the astrocytes of hypertensive rats (**Figure 9**). SP3 proteomic result for GFAP (**Figure 9**) was similar to the microscopic result, representing a significant increase of GFAP in reactive as compared to normal astrocytes. These results of the protein analysis were similar to the study by Hol et al. [31], indicating that an upregulation of GFAP in reactive astrocytes, coincides with neurodegenerative diseases such as HTN. Similarly, a previous study [32] has established that increased levels of GFAP was directly related to hypertension, in SHR. Hence, based on the literature and our study results, it can be concluded that the reactivity in astrocytes could be a direct indicator of hypertension.

The results of our study showed that A1 has both increased levels of GFAP (**Figure 9**) and calpain (**Figure 11**), indicating the increased reactivity in A1 astrocytes may be due to the higher level of calpain, as shown in the previous studies [33, 34], resulting in atherosclerosis and hence HTN [35]. Other studies [36] indicate that calpain can also act on the extracellular substrates, such as collagen-fibronectin, to modulate the cell activity. As calpain can act both intra and extracellularly, it could be a therapeutic target for the prevention of cardiovascular diseases, including hypertension.

In contrast, calpastatin, an endogenous inhibitor of calpain, attenuates its cytotoxicity, thus increasing the levels of calpastatin may be beneficial in the regulation of HTN [25]. The current results show lower expression of calpastatin (**Figure 12**) as compared to calpain (**Figure 11**) in A1 astrocytes, indicating a decreased level of calpastatin in reactive HFAs. These results also suggest that an additional amount of exogenous calpastatin may decrease the toxic activity of calpain, by blocking the active sites of calpain [37]. This remarkable role of calpastatin makes it a promising therapeutic agent for managing blood pressure.

Likewise, another endogenous protease cathepsin, which is involved in inflammatory disorders, was found to be significantly higher (**Figure 13**) in reactive

(A1) astrocytes. Evidence suggests that cathepsin plays an important role in HTN through vascular modulation [38], leading to atherosclerosis. It has also been reported that cathepsin regulates the phosphorylation of mitogen activated protein kinase- kinase (MEK) in Angiotensin II-dependent hypertension [39]. Angiotensin II induces g-protein regulated MAPK cell signalling cycle [40], therefore MAPK was measured in both A1 and A2 astrocytes (**Figure 14**), and it was found to be significantly higher in A1 as compared to A2. This augmented level of MAPK in A1 HFAs could be responsible for the thickening of their intermediate filaments (**Figure 10**), as indicated previously in another study [41] that MAPK upregulates cell proliferation.

In a recent study, the phosphorylation of MAPK in the arteries of hypertensive patients as well as in a mice model [39] was observed. Moreover, the proliferation of arterial smooth muscle cells in both, human and mice models were detected. Thus, a vascular modulatory role of MAPK, which is related to HTN, was confirmed.

Our initial findings based on immunocytochemistry and SP3 proteomic results indicate that identifying molecules such as calpain, calpastatin, cathepsin and MAPK may be useful in reducing the reactivity in the astrocytes, which is an indicator of HTN. The present study shows that in A1, there is an increased levels of calcium gated proteins, possibly due to higher concentration of the intracellular calcium [42, 43], leading to hypertension.

Protein-based therapeutic agents have been highly successful in clinics [44]. More than hundred original and modified therapeutic proteins are used up till now. There are at least five ways of utilising proteins as therapeutic agents:

- a. replacing damaged proteins [45]
- b. augmenting the effects of weak proteins [46]
- c. interfering with an intermediate molecule or its function [47]
- d. providing synthetic molecules for normal function [48]
- e. delivering other compounds or proteins [49]

Further experiments are needed to test these enzymes, using ELISA kits for the specific regulatory proteins, such as S100B, soluble receptor for advanced glycation end product (sRAGE) and GFAP, to identify the most promising predictive biomarker for HTN. The highly specific indicator of astrocytic reactivity, GFAP [50], was measured earlier by immunocytochemistry, proteomics, and now ELISA protocol will be used for further quantification of cytotoxicity due to the higher concentration of GFAP in the reactive astrocytes.

Similarly, the Ca^{2+} -binding protein S100B, acts both intra and extracellularly in HFAs. Inside the cell, S100B acts as a stimulator of proliferation and activation of astrocytes. Whereas, extracellularly, S100B engages sRAGE in pro-proliferative activities [51]. Though, sRAGE might not be the only S100B receptor, and S100B's ability to engage sRAGE might be regulated by its interaction with other calcium-binding proteases, such as calpain, calpastatin, cathepsin and MAPK.

5. Conclusion

This study shows for the first time that reactive astrocytes in HFAs mimic hypertensive conditions, and calcium-dependent proteins such as GFAP, calpain,

calpastatin, cathepsin and MAPK could be considered as potential predictive biomarkers for HTN.

6. Future plans

More experiments are needed for the validation of the predictive biomarkers for HTN. We need to further characterise proteins (S100B, sRAGE and GFAP) in both types of HFAs, using ELISA technique.

Acknowledgements

I would like to thank my supervisors Professor Ann Simpson, Professor Kaneez Fatima Shad and Associate Professor Sara Lal for their constant support and guidance. Special thanks to Associate Professor Louis Cole and Dr. Christian Evenhuis for providing confocal microscopy and OMERO software facilities, to identify peripheral markers of HTN in HFAs, WKY and SHR. I would also like to thank Dr. Matt Padula for providing facilities to perform SP3 experiments and LC/MS/MS detection of HFA-proteins. I would like to acknowledge “Australian Government Research Training Program Scholarship”.

Author details

Fahmida Abdi, Ann M. Simpson, Sara Lal and Kaneez Fatima Shad*
Life Sciences, Faculty of Science, University of Technology Sydney, Sydney,
Australia

*Address all correspondence to: ftmshad@gmail.com

IntechOpen

© 2021 The Author(s). Licensee IntechOpen. This chapter is distributed under the terms of the Creative Commons Attribution License (<http://creativecommons.org/licenses/by/3.0>), which permits unrestricted use, distribution, and reproduction in any medium, provided the original work is properly cited. 

References

- [1] Antonakoudis, G., et al., *Blood pressure control and cardiovascular risk reduction*. Hippokratia, 2007. **11**(3): p. 114-119.
- [2] Shere, A., O. Eletta, and H. Goyal, *Circulating blood biomarkers in essential hypertension: a literature review*. Journal of Laboratory and Precision Medicine, 2017. **2**(12).
- [3] Meissner, A., *Hypertension and the brain: A risk factor for more than heart disease*. Cerebrovascular Diseases, 2016. **42**(3-4): p. 255-262.
- [4] Giles, T., *Biomarkers, cardiovascular disease, and hypertension*. The Journal of Clinical Hypertension, 2013. **15**(1): p. 1-1.
- [5] Li, D.-P. and H.-L. Pan, *Glutamatergic regulation of hypothalamic Presympathetic neurons in hypertension*. Current Hypertension Reports, 2017. **19**(10): p. 78.
- [6] Parsons, M.P. and L.A. Raymond, *Extrasynaptic NMDA receptor involvement in central nervous system disorders*. Neuron, 2014. **82**(2): p. 279-293.
- [7] Gao, M., et al., *1-Aminocyclopropanecarboxylic acid, an antagonist of N-methyl-D-aspartate receptors causes hypotensive and antioxidant effects with upregulation of heme oxygenase-1 in stroke-prone spontaneously hypertensive rats*. Hypertension Research, 2007. **30**(3): p. 249-257.
- [8] Kirchhoff, F., *Analysis of functional NMDA receptors in astrocytes*. Methods Mol Biol, 2017. **1677**: p. 241-251.
- [9] Kommers, T., et al., *Phosphorylation of glial fibrillary acidic protein is stimulated by glutamate via NMDA receptors in cortical microslices and in mixed neuronal/glial cell cultures prepared from the cerebellum*. Brain Res Dev Brain Res, 2002. **137**(2): p. 139-148.
- [10] Marina, N., et al., *Astrocytes monitor cerebral perfusion and control systemic circulation to maintain brain blood flow*. Nature Communications, 2020. **11**(1): p. 131.
- [11] Mishra, A., *Binaural blood flow control by astrocytes: Listening to synapses and the vasculature*. The Journal of physiology, 2017. **595**(6): p. 1885-1902.
- [12] Marina, N., et al., *Control of sympathetic vasomotor tone by catecholaminergic C1 neurones of the rostral ventrolateral medulla oblongata*. Cardiovasc Res, 2011. **91**(4): p. 703-710.
- [13] Verkhratsky, A., R.K. Orkand, and H. Kettenmann, *Glial calcium: Homeostasis and signaling function*. Physiological Reviews, 1998. **78**(1): p. 99-141.
- [14] Araque, A., et al., *Tripartite synapses: Glia, the unacknowledged partner*. Trends Neurosci, 1999. **22**(5): p. 208-215.
- [15] Andres, A.L., et al., *NMDA receptor activation and Calpain contribute to disruption of dendritic spines by the stress neuropeptide CRH*. The Journal of Neuroscience, 2013. **33**(43): p. 16945.
- [16] Hardingham, G.E., Y. Fukunaga, and H. Bading, *Extrasynaptic NMDARs oppose synaptic NMDARs by triggering CREB shut-off and cell death pathways*. Nature Neuroscience, 2002. **5**(5): p. 405-414.
- [17] Hardingham, G.E. and H. Bading, *Synaptic versus extrasynaptic NMDA receptor signalling: Implications for neurodegenerative disorders*. Nature Reviews Neuroscience, 2010. **11**(10): p. 682.

- [18] Wang, Y., et al., *Distinct roles for μ -calpain and m-calpain in synaptic NMDAR-mediated neuroprotection and extrasynaptic NMDAR-mediated neurodegeneration*. The Journal of neuroscience : the official journal of the Society for Neuroscience, 2013. **33**(48): p. 18880-18892.
- [19] Karpova, A., et al., *Encoding and transducing the synaptic or extrasynaptic origin of NMDA receptor signals to the nucleus*. Cell, 2013. **152**(5): p. 1119-1133.
- [20] Krapivinsky, G., et al., *The NMDA receptor is coupled to the ERK pathway by a direct interaction between NR2B and RasGRF1*. Neuron, 2003. **40**(4): p. 775-784.
- [21] Bading, H., *Nuclear calcium signalling in the regulation of brain function*. Nat Rev Neurosci, 2013. **14**(9): p. 593-608.
- [22] Pekny, M. and M. Pekna, *Astrocyte reactivity and reactive astrogliosis: Costs and benefits*. Physiol Rev, 2014. **94**(4): p. 1077-1098.
- [23] Hughes, C.S., et al., *Single-pot, solid-phase-enhanced sample preparation for proteomics experiments*. Nature Protocols, 2019. **14**(1): p. 68-85.
- [24] Adzic, M., et al., *Extracellular ATP induces graded reactive response of astrocytes and strengthens their antioxidative defense in vitro*. Journal of Neuroscience Research, 2017. **95**(4): p. 1053-1066.
- [25] Zhang, S.J., et al., *Nuclear calcium signaling controls expression of a large gene pool: Identification of a gene program for acquired neuroprotection induced by synaptic activity*. PLoS Genet, 2009. **5**(8): p. e1000604.
- [26] Wan, F., et al., *Extracellular Calpain/Calpastatin balance is involved in the progression of pulmonary hypertension*. Am J Respir Cell Mol Biol, 2016. **55**(3): p. 337-351.
- [27] Karpova, A., et al., *Encoding and Transducing the Synaptic or Extrasynaptic Origin of NMDA Receptor Signals to the Nucleus*. Vol. 152. 2013. 1119-33.
- [28] Khakh, B.S. and R.A. North, *Neuromodulation by extracellular ATP and P2X receptors in the CNS*. Neuron, 2012. **76**(1): p. 51-69.
- [29] Boué-Grabot, E. and Y. Pankratov, *Modulation of central synapses by astrocyte-released ATP and postsynaptic P2X receptors*. Neural plasticity, 2017. **2017**: p. 9454275-9454275.
- [30] Neary, J.T., et al., *Extracellular ATP induces stellation and increases glial fibrillary acidic protein content and DNA synthesis in primary astrocyte cultures*. Acta Neuropathologica, 1994. **87**(1): p. 8-13.
- [31] Cho, W. and A. Messing, *Properties of astrocytes cultured from GFAP over-expressing and GFAP mutant mice*. Experimental cell research, 2009. **315**(7): p. 1260-1272.
- [32] Hol, E.M. and M. Pekny, *Glial fibrillary acidic protein (GFAP) and the astrocyte intermediate filament system in diseases of the central nervous system*. Current Opinion in Cell Biology, 2015. **32**: p. 121-130.
- [33] Tomassoni, D., et al., *Increased expression of glial fibrillary acidic protein in the brain of spontaneously hypertensive rats*. Clinical and Experimental Hypertension, 2004. **26**(4): p. 335-350.
- [34] Lee, Y., et al., *Rapid increase in immunoreactivity to GFAP in astrocytes in vitro induced by acidic pH is mediated by calcium influx and calpain I*. Brain research, 2000. **864**: p. 220-229.
- [35] Kim, J.H., et al., *Reactive protoplasmic and fibrous astrocytes contain high levels of calpain-cleaved alpha 2 spectrin*. Exp Mol Pathol, 2016. **100**(1): p. 1-7.

- [36] Miyazaki, T., et al., *M-Calpain induction in vascular endothelial cells on human and mouse atheromas and its roles in VE-cadherin disorganization and atherosclerosis*. *Circulation*, 2011. **124**(23): p. 2522-2532.
- [37] Letavernier, B., et al., *Calpains contribute to vascular repair in rapidly progressive form of glomerulonephritis: Potential role of their externalization*. *Arterioscler Thromb Vasc Biol*, 2012. **32**(2): p. 335-342.
- [38] Wendt, A., V. Thompson, and D. Goll, *Interaction of calpastatin with calpain: A review*. *Biological chemistry*, 2004. **385**: p. 465-472.
- [39] Cheng Xian, W., et al., *Cysteine protease Cathepsins in atherosclerosis-based vascular disease and its complications*. *Hypertension*, 2011. **58**(6): p. 978-986.
- [40] Lu, Y., et al., *Angiotensin II-induced vascular remodeling and hypertension involves cathepsin L/V- MEK/ERK mediated mechanism*. *International Journal of Cardiology*, 2020. **298**: p. 98-106.
- [41] Goldsmith, Z.G. and D.N. Dhanasekaran, *G protein regulation of MAPK networks*. *Oncogene*, 2007. **26**(22): p. 3122-3142.
- [42] Schevzov, G., et al., *Regulation of cell proliferation by ERK and signal-dependent nuclear translocation of ERK is dependent on Tm5NM1-containing actin filaments*. *Molecular biology of the cell*, 2015. **26**(13): p. 2475-2490.
- [43] Hazari, M.A., et al., *Serum calcium level in hypertension*. *North American Journal of Medical Sciences*, 2012. **4**(11): p. 569-572.
- [44] Villa-Etchegoyen, C., et al., *Mechanisms involved in the relationship between low calcium intake and high blood pressure*. *Nutrients*, 2019. **11**(5): p. 1112.
- [45] Dimitrov, D.S., *Therapeutic proteins*. *Methods in molecular biology* (Clifton, N.J.), 2012. **899**: p. 1-26.
- [46] Gorzelany, J.A. and M.P. de Souza, *Protein Replacement Therapies for Rare Diseases: A Breeze for Regulatory Approval? Science Translational Medicine*, 2013. **5**(178): p. 178fs10.
- [47] Carter, P.J., *Introduction to current and future protein therapeutics: A protein engineering perspective*. *Experimental Cell Research*, 2011. **317**(9): p. 1261-1269.
- [48] Baker, M.P. and T.D. Jones, *Identification and removal of immunogenicity in therapeutic proteins*. *Current opinion in drug discovery & development*, 2007. **10**(2): p. 219-227.
- [49] Goeddel, D.V., et al., *Expression in Escherichia coli of chemically synthesized genes for human insulin*. *Proceedings of the National Academy of Sciences*, 1979. **76**(1): p. 106.
- [50] Emi Aikawa, N., et al., *Immunogenicity of anti-TNF- α agents in autoimmune diseases*. *Clinical Reviews in Allergy & Immunology*, 2010. **38**(2): p. 82-89.
- [51] Middeldorp, J. and E.M. Hol, *GFAP in health and disease*. *Progress in Neurobiology*, 2011. **93**(3): p. 421-443.